S-Nitrosation and Regulation of Inducible Nitric Oxide Synthase†

Douglas A. Mitchell,‡ Phillip A. Erwin,§ Thomas Michel,§,|| and Michael A. Marletta*,‡,⊥,#

Department of Chemistry, Department of Molecular and Cell Biology, and Division of Physical Biosciences, Lawrence Berkeley National Laboratory, University of California, Berkeley, Berkeley, California 94720-1460, Cardiovascular Division, Brigham and Women's Hospital, Harvard Medical School, Boston, Massachusetts 02115, and VA Boston Healthcare System, West Roxbury, Massachusetts 02132

Received December 6, 2004; Revised Manuscript Received January 31, 2005

ABSTRACT: The inducible isoform of nitric oxide synthase (iNOS) and three zinc tetrathiolate mutants (C104A, C109A, and C104A/C109A) were expressed in *Escherichia coli* and purified. The mutants were found by ICP-AES and the zinc-specific PAR colorimetric assay to be zinc free, whereas the wild-type iNOS zinc content was 0.38 ± 0.01 mol of Zn/mol of iNOS dimer. The cysteine mutants (C104A and C109A) had an activity within error of wild-type iNOS (2.24 ± 0.12 μmol of NO min^{-1} mg^{-1}), but the double cysteine mutant had a modestly decreased activity (1.75 ± 0.14 μmol of NO min^{-1} mg^{-1}). To determine if NO could stimulate release of zinc and dimer dissociation, wild-type protein was allowed to react with an NO donor, DEA/NO, followed by buffer exchange. ICP-AES of samples treated with 10 μM DEA/NO showed a decrease in zinc content (0.23 ± 0.01 to 0.09 ± 0.01 mol of Zn/mol of iNOS dimer) with no loss of heme iron. Gel filtration of wild-type iNOS treated similarly resulted in ∼20% more monomeric iNOS compared to a DEA-treated sample. Only wild-type iNOS had decreased activity (42 ± 2%) after reaction with 50 μM DEA/NO compared to a control sample. Using the biotin switch method under the same conditions, only wild-type iNOS had increased levels of S-biotinylation. S-Biotinylation was mapped to C104 and C109 on wild-type iNOS using LysC digestion and MALDI-TOF/TOF MS. Immunoprecipitation of iNOS from the mouse macrophage cell line, RAW-264.7, and the biotin switch method were used to confirm endogenous S-nitrosation of iNOS. The data show that S-nitrosation of the zinc tetrathiolate cysteine results in zinc release from the dimer interface and formation of inactive monomers, suggesting that this mode of inhibition might occur in vivo.

Nitric oxide synthase (NOS, EC 1.14.13.39) catalyzes the oxidation of L-arginine to citrulline and NO.[1] In the first step of the NOS reaction, arginine undergoes N-hydroxylation at one of the terminal guanidino nitrogens, leading to the formation of N^G-hydroxy-L-arginine (NHA) as an intermediate (*1*, *2*). Subsequent oxidation of NHA at the oxime nitrogen yields citrulline and NO. The overall reaction is a five-electron oxidation that consumes NADPH and O_2 in both steps and requires heme (*3*−*5*), FMN, FAD (*6*−*8*), and H_4B (*8*−*10*) as enzyme-bound cofactors. Three isoforms of NOS have been characterized in mammals, and each is a distinct gene product differing in subcellular localization, tissue distribution, and mode of regulation (*10*, *11*). All are homodimeric, require an associated CaM for turnover (*12*, *13*), and probably share a common mechanism even though there are some isoform-specific differences in catalysis. Each NOS has a heme-containing oxygenase domain and a flavoprotein reductase domain (*14*). The enzyme active site is contained entirely within the heme domain, which also binds substrate (arginine or NHA) and H_4B (*15*, *16*). The reductase domain binds NADPH, FMN, and FAD and serves to provide electrons to the active site for catalysis (*17*, *18*).

† This work is supported in part by grants from the NIH to T.M. (GM 36259 and HL46457) and the DeBenedictis Fund of UC Berkeley to M.A.M. P.A.E. is supported by a predoctoral fellowship from the Howard Hughes Medical Institute.

* To whom correspondence should be addressed at the Department of Chemistry, University of California, Berkeley, 211 Lewis Hall, Berkeley, CA 94720-1460. Phone: (510) 643-9325. Fax: (510) 643-9388. E-mail: marletta@berkeley.edu.

‡ Department of Chemistry, University of California, Berkeley.

§ Brigham and Women's Hospital, Harvard Medical School.

|| VA Boston Healthcare System.

⊥ Department of Molecular and Cell Biology, University of California, Berkeley.

Division of Physical Biosciences, Lawrence Berkeley National Laboratory, University of California, Berkeley.

[1] Abbreviations: iNOS, murine macrophage inducible nitric oxide synthase; $iNOS_{heme}$, heme domain of inducible nitric oxide synthase; cNOS, constitutive isoforms of NOS; CaM, calmodulin; BSA, bovine serum albumin; oxyHb, oxyhemoglobin; HRP, horseradish peroxidase; H_4B, (6*R*)-5,6,7,8-tetrahydro-L-biopterin; NADPH, reduced nicotinamide adenine dinucleotide phosphate; NO, nitric oxide; SDS−PAGE, sodium dodecyl sulfate−polyacrylamide gel electrophoresis; PBS, phosphate-buffered saline; FBS, fetal bovine serum; LPS, lipopolysaccharide; IFN, interferon; IPTG, isopropyl β-D-thiogalactopyranoside; ALA, δ-aminolevulinic acid; HEPES, 4-(2-hydroxyethyl)-1-piperazineethanesulfonic acid; TFA, trifluoroacetic acid; LysC, *Lysobacter enzymogenes* endoproteinase Lys-C; AspN, *Pseudomonas fragi* mutant endoproteinase Asp-N; biotin-HPDP, *N*-[6-(biotinamido)hexyl]-3′-(2′-pyridyldithio)propionamide; MMTS, methyl methanethiosulfonate; EDTA, ethylenediamine-*N*,*N*,*N*′,*N*′-tetraacetic acid; PAR, 4-(2-pyridylazo)resorcinol; HCCA, α-cyano-4-hydroxycinnamic acid; Ni-NTA, nickel nitrilotriacetic acid agarose; DTT, dithiothreitol; DMF, *N*,*N*-dimethylformamide; MeCN, acetonitrile; DEA, diethylamine; DEA/NO, diethylammonium (*Z*)-1-(*N*,*N*-diethylamino)diazen-1-ium-1,2-diolate; HPLC, high-performance liquid chromatograpy; MS, mass spectrometry; MALDI, matrix-assisted laser desorption/ionization; TOF, time of flight; CID, collision-induced dissociation; UV−vis, ultraviolet−visible spectrophotometry; ICP-AES, inductively coupled plasma atomic emission spectrometry.

10.1021/bi0474463 CCC: $30.25
Published on Web 03/04/2005

H_4B and L-arginine binding (*19*, *20*), CaM association (*21*, *22*), and a zinc tetrathiolate cluster (*23*−*25*) all contribute to the stabilization of homodimeric NOS; monomeric NOS is inactive (*26*). Two cysteines from each heme domain (C104 and C109) contribute thiol moieties to this cluster, which is commonly viewed as only playing a structural role. Recent reports in the literature highlight the extraordinary reactivity of cysteines involved in zinc ligation toward electrophiles, including N_2O_3 (an intermediate in the primary aqueous decomposition pathway of NO), which would yield a nitrosothiol (*27*−*30*). Zn^{2+} is a Lewis acid, and ligation to cysteine in the form of a zinc tetrathiolate cluster dramatically reduces the pK_a of the thiol, allowing the much more nucleophilic thiolate to predominate at physiological pH (*31*, *32*). The increased nucleophilicity of the cysteines in the cluster, combined with the structural importance of the zinc tetrathiolate for dimer formation and, therefore, activity, suggests that modification of the cluster might lead to altered function. The reactivity of the zinc tetrathiolate cysteines of endothelial NOS has been previously shown to be sensitive to peroxynitrite oxidation (*33*). However, in the absence of superoxide, or when substoichiometric amounts of superoxide are present, two potential electrophiles that could react with the thiolates of NOS are NO or N_2O_3. Formation of N_2O_3 within the macrophage is likely due to the high concentration of NO used for pathogen killing (*34*, *35*). Concentrations of NO used in signaling lead to very low concentrations of N_2O_3, but nitrosothiols could still be formed by nucleophilic attack on NO with subsequent one-electron oxidation (*36*) or oxidation of the thiolate to a thiyl radical with direct radical recombination with NO (*37*).

Here, we investigate the possibility that S-nitrosation of the zinc tetrathiolate cysteines of iNOS plays a regulatory role by virtue of their importance in homodimer stability and increased nucleophilicity. Using the biotin switch method (*38*), proteolytic digestion, and MALDI MS, we show that NO in aerobic solution reacts with high selectivity with the zinc tetrathiolate cysteines of iNOS. S-Nitrosation of the cysteines originally involved in zinc ligation leads to zinc release from the dimer interface and the dissociation of NOS into inactive monomers. It has long been known that exposure of NOS to NO lowers the activity of NOS (*39*−*41*). More recently, overexpression of the primary intracellular protein reductant, thioredoxin, was shown to prevent reduction in NOS activity (*42*, *43*). The work reported here suggests that the mechanism of NO-mediated inhibition of iNOS can be explained by S-nitrosation of the zinc tetrathiolate cysteines and that iNOS expressed in an activated macrophage is isolated with a portion S-nitrosated. The S-nitrosated enzyme that has dissociated into monomeric form will remain inactive until either reduction of the key cysteines and re-formation of the zinc tetrathiolate or formation of an interchain NOS disulfide. Both of these routes would lead to the active dimeric species. This study has ramifications on our current understanding of posttranslational control of NO production. This regulation may be especially important for the full comprehension of the role of iNOS in chronic inflammation and infection.

EXPERIMENTAL PROCEDURES

Materials. H_4B was from Schircks Laboratories. Pefabloc SC hydrochloride and sequencing grade trypsin, LysC, and AspN were from Roche Diagnostics. IPTG and *Escherichia coli* JM109 competent cells were purchased from Promega. *E. coli* DH5α competent cells and terrific broth were from Life Technologies. Ni-NTA and the QIAprep miniprep kit were from Qiagen. The 2′,5′-ADP Sepharose 4B resin, S200 16/60 gel filtration column, and PD-10 desalting columns were purchased from Amersham Biosciences. The Emulsi-Flex-C5 high-pressure homogenizer was from Avestin, Inc. C-18 ZipTips and centrifugal filtration units (Ultrafree-15, Biomax-50K NMWL membrane) were from Millipore. Precast Novex 10−20% Tris−glycine gels, Dulbecco's modified Eagle's medium, penicillin, streptomycin, Mark 12, and SeeBlue Plus2 molecular mass standards were from Invitrogen. Protran BA nitrocellulose transfer membranes were from Schleicher & Schuell. Biotin-HPDP, MMTS, SuperSignal West femto maximum sensitivity substrate, NeutrAvidin-HRP conjugate, and immobilized streptavidin were from Pierce. Anti-iNOS monoclonal and polyclonal antibodies were from BD Transduction Labs. RAW-264.7 cells were from the ATCC. *E. coli* lipopolysaccharide and recombinant murine IFN-γ were from Calbiochem. FBS was from Hyclone. DEA/NO was from Cayman Chemical. Protein assay dye reagent concentrate and Coomassie Blue R-250 were purchased from Bio-Rad. The QuikChange site-directed mutagenesis kit was from Stratagene. All other reagents were purchased from Sigma-Aldrich.

General Methods. The Bradford assay was used for the quantification of all proteins in this study. All electronic absorbance spectra were collected using a Cary 3E spectrophotometer at 22 °C unless otherwise indicated. Metal analysis was performed on a Perkin-Elmer 3000DV ICP-AES using commercially available metal standard solutions. All buffers used in this study were prepared using >18 MΩ water and did not have detectable iron, cobalt, zinc, nickel, or manganese by ICP-AES.

Site-Directed Mutagenesis of iNOS. The iNOS mutant constructs were made using the Stratagene QuikChange method. The mutagenesis primers were synthesized by Elim Biopharmaceuticals (Hayward, CA) and were HPLC purified. For the iNOS C104A mutant, the following primers were used: sense, 5′-GGC CAC ATC GGA TTT CAC TGC AAA GTC CAA GTC TTG CTT GG-3′; antisense, 5′-CCA AGC AAG ACT TGG ACT TTG CAG TGA AAT CCG ATG TGG CC-3′. For the iNOS C109A mutant, the following primers were used: sense, 5′-CAC TTG CAA GTC CAA GTC TGC GTT GGG GTC CAT CAT GAA CC-3′; antisense, 5′-GGT TCA TGA TGG ACC CCA ACG CAG ACT TGG ACT TGC AAG TG-3′. The plasmid encoding the C104A mutant was arbitrarily chosen to prepare the C104A/C109A double mutant, and the following primers were used: sense, 5′-CAC TGC CAA GTC CAA GTC TGC ATT GGG GTC CAT CAT GAA CC-3′; antisense, 5′-GGT TCA TGA TGG ACC CCA ATG CAG ACT TGG ACT TGG CAG TG-3′. The plasmid DNA was sequenced by the UC Berkeley DNA Sequencing Facility to verify the presence of the mutation.

Expression and Purification of iNOS. Expression and purification of the wild-type and cysteine mutant full-length proteins were carried out in *E. coli*, under the control of an IPTG-inducible promoter, as described previously with minor modifications (*44*). All cultures were grown to an optical density of ∼0.6 and induced for 23 h at 22 °C using 1 mM

IPTG in the presence of 1 mM ALA. All buffers used in the lysis, purification, and concentration steps contained 10 μM H_4B. Cell pellets from 3 L of culture were resuspended in lysis buffer containing 50 mM HEPES (pH 7.4), 10% glycerol, 1 mM Pefabloc SC, 10 μg/mL benzamidine, 5 μg/mL leupeptin, and 1 μg/mL each of pepstatin, chymostatin, and antipain. The resuspended cells were lysed with an Avestin EmulsiFlex-C5 high-pressure homogenizer. Centrifugation for 1 h at 42000 rpm yielded supernatant that was immediately purified using 2′,5′-ADP-Sepharose affinity chromatography as previously described (*44*). The eluate was concentrated using a centrifugal filtration device and loaded onto a gel filtration column (Superdex 200 HiLoad 26/60), which was equilibrated with 100 mM HEPES (pH 7.4), 100 mM NaCl, 10 μM H_4B, and 10% glycerol. Fractions containing the iNOS dimer were pooled, concentrated, and frozen in aliquots at −80 °C. iNOS purified in this manner is typically >95% pure as judged by SDS−PAGE and UV−vis. Adequate heme incorporation into the protein was verified by the A_{280}/A_{415} ratio (*45*). Yields range from 5 to 6 mg/L of culture and were determined using the Bradford protein assay with a BSA standard.

Purification of iNOS$_{heme}$. The construct encoding the heme domain of iNOS (residues 1−490) has a C-terminal $(His)_6$ tag and was expressed in an identical manner as the full-length protein. Purification of $iNOS_{heme}$ was achieved as previously described except for the elimination of the final anion-exchange column (*45*). The heme domain of iNOS was purified by metal affinity (Ni-NTA) and gel filtration (Superdex 200 HiLoad 26/60). The proteins prepared with or without the final anion-exchange step were indistinguishable by SDS−PAGE. Adequate heme incorporation into the protein was verified by the A_{280}/A_{428} ratio (A_{428} corresponds to the Soret maximum from a heme−imidazole complex).

Oxyhemoglobin Assay. The specific activity of the wild-type and mutant iNOS proteins (15 nM) was determined in triplicate using the oxyHb assay. NO produced by iNOS can be measured by monitoring the rapid oxidation of oxyHb by NO. This reaction generates methemoglobin and nitrate and was performed as previously described (*46*).

Analytical Gel Filtration. A Superdex 200 HiLoad 16/60 gel filtration column was used to test whether iNOS as purified (exclusively homodimer) would dissociate into monomers in response to the NO donor, DEA/NO. In a typical reaction, 4 μM iNOS in 1 mL of 100 mM HEPES (pH 7.4) was reacted with 0, 10, or 100 μM DEA or DEA/NO for 20 min at 37 °C. Under these conditions, all NO has been released from DEA/NO (1.5 equiv). The entire reaction mixture was then loaded onto the column, which was kept at 4 °C for the duration of the experiment.

PAR Assay. A zinc-specific dye, PAR, was used to spectrophotometrically determine the concentration of free zinc in solution. PAR is yellow (λ_{max} = 400 nm) and binds zinc in a 2:1 stoichiometry with an absorbance shift to 500 nm. A stock solution of 200 μM PAR was prepared in 50 mM HEPES (pH 7.0) and 100 mM NaCl. Determination of free zinc in solution was performed as follows: the UV−vis spectrophotometer was blanked on 8 μM PAR in 200 μL of PAR assay buffer in a quartz cuvette. After thorough washing of the cuvette, the sample for zinc analysis was dissolved into a solution of 8 μM PAR in assay buffer. The solution was then diluted to a total volume of 200 μL and given approximately 5 min to attain equilibrium, and then the spectrum was acquired.

Preparation of Biotinylated iNOS$_{heme}$. The heme domain of iNOS was S-biotinylated by reaction with a reductively labile, thiol-specific biotinylating reagent (biotin-HPDP) to provide a positive control for the biotin switch method and to assess the sensitivity of the Western blot. Biotin-HPDP (37 μL of a 4 mM stock in DMF) was reacted with 1.6 mg of purified $iNOS_{heme}$ in a 500 μL volume of PBS (pH 7.4). This solution was allowed to react for 90 min at 37 °C, and the reaction progress was monitored by the increase in A_{343}. The byproduct of the reaction of biotin-HPDP with a thiol is pyridine-2-thione (ϵ_{343} = 8080 M^{-1} cm^{-1}). Excess biotin-HPDP was removed on a PD-10 desalting column. The final concentration of the S-biotinylated $iNOS_{heme}$ after addition of 10% glycerol was found to be 0.83 mg/mL by UV−vis. The stock solution was stored at −80 °C in small aliquots until needed. Biotinylation of $iNOS_{heme}$ was confirmed by running dilutions of this sample on a denaturing 10−20% Tris−glycine gel using nonreducing loading buffer. The gel was then transferred by electroblot to a nitrocellulose membrane. The membrane was blocked for 12 h in 30 mL of PBS with 0.05% Tween 20 and 3% BSA. The solution was then replaced with 30 mL of fresh PBS/Tween/BSA solution, and the NeutrAvidin-HRP conjugate (1:10000 dilution) was allowed to bind for 1 h at room temperature with gentle agitation. The membrane was then washed for 10 min, three times, with ∼30 mL of PBS/Tween. A mixture of 2 mL of West femto substrate and 2 mL of enhancer solution was reacted with the membrane for 5 min. A Bio-Rad Fluor-S MultiImager was used for chemiluminescence detection.

Biotin Switch Method on E. coli Expressed iNOS. The biotin switch method was employed to assay for S-nitrosation of iNOS, $iNOS_{heme}$, and all of the cysteine mutants. This assay exchanges a photolabile nitrosothiol with a disulfide-linked biotin. The biotin tag serves as a primary antibody for Western blotting, a purification handle, and extra mass for mapping the modified cysteine by MS. The assay was performed as previously described with some modifications (*38*). The initial protein concentration was 0.5 μg/μL, and reactions were in a 125 μL total volume. For the first step of the assay, DEA/NO and the appropriate negative control (DEA) were used at a concentration of 50 μM in 25 mM HEPES (pH 7.4) using >18 MΩ water, which had no detectable metals. The buffer for the rest of the assay included EDTA (100 μM) and neocuproine (10 μM) to ensure that nondetectable metal-catalyzed nitrosothiol decomposition would be minimized. If metal chelators are present during the S-nitrosation step, the zinc from the zinc tetrathiolate cluster of iNOS could be removed. Acetone precipitations were used to remove the aqueous decomposition products of DEA/NO, MMTS, DMF, and biotin-HPDP in each step of the switch assay. We have noticed that failure to remove the relatively high amount of DMF before SDS−PAGE can lead to streaking and/or bending in the gel. This results in a poor quality Western blot.

Anaerobic Biotin Switch Method. The first step in the biotin switch method, in vitro S-nitrosation, was also performed anaerobically. This was accomplished by deoxygenating the metal chelator free buffer by 10 cycles of vacuum and argon purging on a gas manifold system in a gastight vial. This buffer, along with iNOS (15 mg/mL) and

DEA/NO or DEA (9 mM in 100 mM aqueous NaOH) stock solutions, was placed in an anaerobic chamber. The reaction setup was identical to that of the aerobic samples except that these samples were kept anaerobic until the NO donor had completed 10 half-lives of decomposition (~20 min). Acetone used in the first precipitation was sparged with nitrogen for 10 min to minimize the concentration of dissolved oxygen. The remainder of the biotin switch method was performed as described above.

Proteolytic Digests and MALDI-TOF MS Analysis of Peptide Fragments. Purified iNOS (20 μg) was diluted to 30 μL in PBS (pH 7.4). Digestions were initiated with the addition of 100 ng of trypsin (1:200), 267 ng of AspN (1:75), or 267 ng of LysC (1:75). The mixtures were incubated at 37 °C for 5 h. Samples for MALDI MS were desalted using C-18 ZipTips and were eluted with 9 μL of a 50% MeCN:49.9% H_2O:0.1% TFA solution saturated with HCCA (~10 mg/mL). The matrix/peptide solution (1 μL) was spotted onto the MALDI target. Spectra were acquired in reflector mode over the range *m*/*z* 600−5000 Da using an Applied Biosystems Voyager-DE PRO mass spectrometer. The instrument was internally calibrated using four peptides from the digest of known molecular mass flanking the peptide of interest.

Purification of Biotinylated Peptides with Streptavidin−Agarose. Immobilized streptavidin (agarose beads) was used to confirm the presence of biotinylated peptide fragments from the proteolytic digests described above using iNOS protein that had undergone the biotin switch method. iNOS peptides were added after equilibration of the beads in PBS. The suspended slurry (50 μL) was centrifuged for 2 min at 8000 rpm in a 0.6 mL microcentrifuge tube. The solution was decanted, and the beads were washed twice with 100 μL of PBS using centrifugation to pellet the beads between washings. An aliquot of the above digests (10 μL) was then diluted to 50 μL in PBS and applied to the immobilized streptavidin. The peptides were allowed to bind for 45 min at room temperature with agitation provided by a vortexer on low power. Centrifugation for an additional 2 min at 8000 rpm pelleted the beads with the biotinylated peptides bound, and the nonbiotinylated peptides were decanted. Weak and nonspecific binders to streptavidin and/or agarose were removed by 3 × 100 μL PBS wash/centrifuge/decant rounds and 2 × 100 μL rounds using >18 MΩ H_2O. Biotinylated peptides were eluted using approximately 30 μL of 50% MeCN:49.9% H_2O:0.1% TFA with heating at 80 °C for 2 min with vortexing. An aliquot of this solution (1 μL) was diluted into 10 μL of the saturated HCCA solution described above and analyzed by MALDI MS.

MS/MS Analysis of LysC-Digested iNOS. iNOS was digested with LysC following the above protocol. Peptides from the digest solution were adsorbed onto a C-18 ZipTip and eluted with 4 μL of 50% MeCN:49.9% H_2O:0.1% TFA. A 0.7 μL aliquot of this solution was mixed with an equal volume of saturated HCCA (~10 mg/mL) in the same solvent and allowed to dry on the MALDI target. A full-scan mass spectrum of the digest was recorded on an AB 4700 MALDI tandem TOF instrument in reflector mode over the range *m*/*z* 600−4500 Da; then the protonated peptide ions at *m*/*z* 1300.5 and 1477.7 Da were then isolated in MS1, and individual CID spectra were acquired. Air was used as the collision gas at 1.0 keV (lab frame) collision energy.

Cell Culture. RAW-264.7 cells were maintained in Dulbecco's modified Eagle's medium supplemented with 10% (v/v) FBS, 2% penicillin, and 2% streptomycin at 37 °C. These cells were activated for 24 h with *E. coli* LPS (35 ng/mL) plus recombinant murine IFN-γ (5 units/mL).

Preparation of Macrophage Lysates, Immunoprecipitation, and Biotin Switch. After activation, each 100 mm dish of macrophages was lysed by scraping cells into 1 mL of lysis buffer comprised of Tris (20 mM, pH 7.4), NP-40 (1% v/v), deoxycholate (2.5% w/v), NaCl (150 mM), Na_3VO_4 (2 mM), EDTA (1 mM), NaF (1 mM), and neocuproine (100 μM) supplemented with a mixture of protease inhibitors. Lysates were rocked at 4 °C for 30 min and centrifuged at 14000*g* for 15 min. The supernatants were then incubated with 4 μg of anti-iNOS polyclonal antibody for 1 h at 4 °C with rocking. After addition of immobilized protein A (agarose beads) and another hour of rocking at 4 °C, the beads were washed extensively with lysis buffer, and iNOS was eluted from the beads. After iNOS elution, nitrosothiols were reduced by adding 4 volumes of a solution comprised of $HgCl_2$ (3 mM), HEPES (250 mM, pH 7.7), neocuproine (100 μM), and SDS (2.5%) and kept at 40 °C for 30 min with shaking and frequent vortexing. The same solution without $HgCl_2$ was used as a control. iNOS was then precipitated with 1 volume of acetone, incubated at −20 °C for 30 min, and centrifuged at 14000*g* for 30 min. The pellet was washed with cold acetone, resuspended in HEPES (250 mM, pH 7.7), EDTA (1 mM), neocuproine (100 μM), and SDS (1%), and subjected to the biotin switch method as above. After another acetone precipitation, S-biotinylated iNOS was trapped with streptavidin−agarose, eluted, and resolved by SDS−PAGE. All steps before biotinylation were performed under low-light conditions. Proteins were electroblotted onto nitrocellulose membranes, and an anti-iNOS monoclonal antibody was used to probe immunoblots, which were processed as described previously (*47*).

RESULTS

Purification of iNOS, Cysteine Mutants, and iNOS$_{heme}$. All of the iNOS proteins expressed in *E. coli* were purified to >95% as judged by Coomassie-stained SDS−PAGE (shown in Supporting Information). A UV−vis spectrum was taken for each protein to ensure adequate heme incorporation. For the full-length constructs, the ratio of A_{280}/A_{415} was in the range 2.5−2.6. For the heme domain construct, the $A_{280}/A_{428} = 1.4$.

The last step in each purification involved gel filtration, and although we observed some proteolysis evidenced by the appearance of the reductase domain, no monomeric protein was detected, even in the cysteine mutants (data not shown). The proteolytically generated reductase domain is in accord with previous studies involving NOS overexpression in *E. coli* (*48*). Finding only dimeric protein in the double cysteine mutant, C104A/C109A, was unexpected because this mutant was anticipated to have very low or no affinity for zinc and is also incapable of forming an interchain disulfide (reducing agents were not added to the gel filtration running buffer). It appears that other contacts at the dimer interface are sufficient to keep the protein dimeric at high protein concentration (~20 mg/mL, 150 μM) and low temperature (4 °C) used while purifying the double mutant.

Table 1: ICP-AES Analysis of Fe and Zn Content[a]

protein sample	Fe content	Zn content
iNOS	1.25 ± 0.01	0.38 ± 0.01
iNOS C104A	1.06 ± 0.01	<0.08
iNOS C109A	1.03 ± 0.01	<0.08
iNOS C104A/C109A	1.08 ± 0.01	<0.08
$iNOS_{heme}$	1.27 ± 0.01	0.46 ± 0.06

[a] Several iNOS proteins were purified from an *E. coli* expression system, and the metal content was analyzed by ICP-AES, 7.2 μM iNOS injection. Iron and zinc content is represented as equivalents of metal per monomer; therefore, full incorporation of iron is 1.00 and for zinc is 0.50. Error in the measurement is expressed as standard deviation and is from three separate measurements. The detection limit for Zn is 0.08 equiv per iNOS monomer.

Zinc Content of iNOS Cysteine Mutants. To determine if the mutant iNOS proteins (C104A, C109A, and C104A/C109A) were capable of zinc binding, ICP-AES was employed. Iron content from the heme cofactor was also quantified and served as an internal benchmark for zinc incorporation (Table 1). Wild-type iNOS and the heme domain both have zinc bound (0.38 ± 0.01 and 0.46 ± 0.06 mol of Zn/mol of monomer, respectively) whereas the cysteine mutants did not show any zinc binding within the detection limit of the instrument (~40 μg/L). As described in earlier work from this laboratory (*45*) and others (*15*, *49*), a typical overexpression of NOS in *E. coli* will yield less than the maximum zinc ion content (0.5 mol of Zn/mol of monomer). Full zinc incorporation is only attainable upon the addition of exogenous reducing agents and $ZnCl_2$ (*24*). The crystal structures of dimeric isoforms of the NOS heme domain have been solved with and without an intact zinc tetrathiolate cluster. In the apoprotein, disulfides between the heme domains assist in dimer stabilization. However, it is widely believed that the in vivo form of NOS contains zinc (*25*, *50*).

Zinc Content by the PAR Assay. To confirm results from ICP-AES, the PAR assay was used. The zinc-binding dye, PAR, has been reported in the literature to form a PAR_2−zinc complex with $\epsilon_{500} = 69\ mM^{-1}\ cm^{-1}$ at pH 7.8 (*30*, *51*). Under the conditions employed here (pH 7.0), the PAR_2−zinc complex has a lower extinction coefficient of $\epsilon_{500} = 45.6\ mM^{-1}\ cm^{-1}$. Free zinc concentrations as low as 200 nM were reproducibly quantified under these conditions. To determine if PAR was able to remove zinc from native protein samples, we assayed the following samples in PAR assay buffer: 2 μM carbonic anhydrase (2 μM zinc), 1 μM superoxide dismutase (2 μM zinc), 1 μM alcohol dehydrogenase (2 μM zinc), and 4 μM wild-type iNOS (2 μM zinc). No free zinc was detected in any of these samples (data not shown). To ensure that the dye is able to bind zinc in the presence of a denatured protein, the above samples were boiled in 1% SDS for 5 min and spectra were reacquired. In each case, the dye complex was formed reproducibly within 15% of the expected zinc concentration (data not shown). The maximum error of 15% may be accounted for by the possibility that these proteins were purified without 100% zinc incorporation. It is important to note that, upon denaturation, iNOS releases all bound cofactors. Beer's plots of all of the cofactors from iNOS revealed that only the heme absorbs at 500 nm under our assay conditions ($\epsilon_{500} = 8400\ M^{-1}\ cm^{-1}$; data not shown). Since 500 nm is the visible maximum of the dye complex, the contribution from heme was subtracted when quantifying the concentration of zinc. The PAR assay was then repeated on the three iNOS mutants after denaturation. No dye complex was observed (data not shown). This is in agreement with ICP-AES measurements.

Table 2: Activity of All of the Full-Length iNOS Proteins Expressed from *E. coli* As Measured by the oxyHb Assay[a]

protein sample	specific activity[b]
iNOS	2.24 ± 0.12
iNOS C104A	2.21 ± 0.16
iNOS C109A	2.37 ± 0.14
iNOS C104A/C109A	1.75 ± 0.14

[a] The oxyHb assay was used to measure the activity of the wild type and cysteine mutants of iNOS (15 nM) at 37 °C. The proteins were kept at 4 °C until addition into the cuvette. [b] The specific activity is expressed as μmol of NO $min^{-1}\ mg^{-1}$ and determined by monitoring an increase in A_{401} (metHb). The error is expressed as standard deviation and is from three separate measurements.

Activity of iNOS and Cysteine Mutants. The activity of all full-length iNOS proteins was measured using the oxyHb assay (Table 2). Wild-type iNOS had the same activity as both single cysteine mutants (C104A and C109A); however, the double cysteine mutant activity was decreased by 20−25%. As noted above, none of the mutants have detectable zinc whereas the zinc content of the wild-type protein was as expected for recombinantly expressed protein. Since analytical gel filtration confirmed that the mutants were dimeric as purified (high concentration and 4 °C), it was not surprising to see significant catalytic activity in all of the proteins since they were maintained at 4 °C prior to the assay.

Effect of DEA/NO on Monomerization of iNOS and Zinc Release. To determine if iNOS dimer stability could be altered by the addition of a NO donor, purified wild-type iNOS was treated with DEA/NO in the dark at 37 °C for 20 min. As a control, the protein was treated with the amine decomposition product of DEA/NO (DEA), also in the dark. As seen in Figure 1, dimer stability is affected by warming the protein to 37 °C for 20 min. Samples treated with DEA (10 or 100 μM) under the same conditions showed no visible increase in monomer formation. The dimer content is estimated to be 60% of the total protein in each of these controls. This is in contrast to samples treated with increasing concentrations of DEA/NO. In the samples treated with 10 μM DEA/NO for 20 min at 37 °C, the dimer content is estimated at 40%. After reaction with 100 μM DEA/NO, estimating the dimer content becomes more difficult due to protein aggregation in the sample. However, the concentration of dimer in the 100 μM sample is visibly lower than in the 10 μM sample, approximately 20% of the total protein.

To determine if zinc was lost during the reaction with the NO donor, the reactions of iNOS with 10 μM DEA and 10 μM DEA/NO were repeated as above. After buffer exchange (dilution factor ~1600) using a 30 kDa molecular mass cutoff Millipore centricon (4 °C, 3000 rpm), the samples were subjected to ICP-AES (Table 3). Zinc content in the buffer and DEA-treated samples was decreased from that in iNOS as isolated. This is in agreement with the analytical gel filtration results: warming promotes monomer formation. Reaction with a NO donor releases zinc to a level well below the controls after buffer exchange.

Effect of DEA/NO on Activity of iNOS and Cysteine Mutants. The oxyHb assay was utilized to quantify any

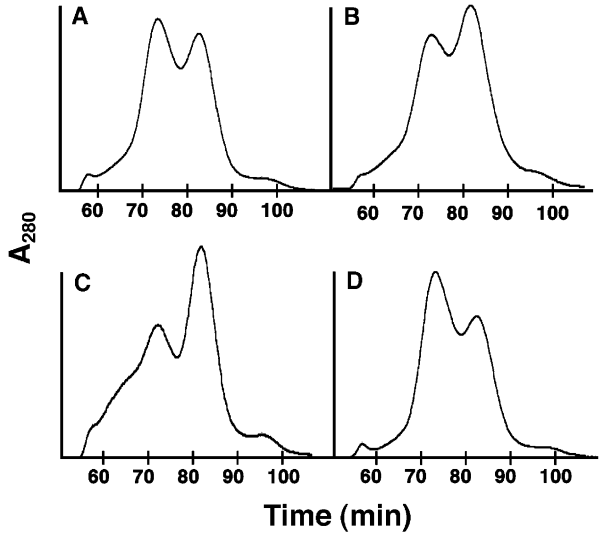

FIGURE 1: A_{280} traces from Superdex 200 HiLoad 16/60 analytical gel filtration of wild-type iNOS. Dimeric iNOS elutes first (leftmost peak) with the monomer following shortly thereafter. All samples were placed at 37 °C for 20 min before chromatography was initiated. (A) iNOS alone. (B) iNOS with 10 μM DEA/NO. (C) iNOS with 100 μM DEA/NO. Aggregation is visible in the earlier time points of the trace. (D) iNOS with 100 μM DEA. The trace for 10 μM DEA was identical to trace D.

Table 3: Metal Content of iNOS Measured by ICP-AES after DEA/NO-Stimulated Dimer Dissociation and Buffer Exchange[a]

protein sample	Fe content	Zn content
iNOS + buffer	1.00 ± 0.04	0.22 ± 0.01
iNOS + 10 μM DEA	1.12 ± 0.04	0.23 ± 0.01
iNOS + 10 μM DEA/NO	1.11 ± 0.01	0.09 ± 0.01

[a] Zinc and iron content was analyzed by ICP-AES on wild-type iNOS (7.2 μM injection) after reaction with buffer, DEA, and DEA/NO. After the NO donor was fully decomposed to DEA and NO (~20 min at 37 °C), the samples were buffer exchanged using a 30 kDa cutoff centricon (Millipore) to remove any released metal. The metal content is expressed as equivalents per monomer with the error expressed as standard deviation from three separate measurements.

differences in activity after reaction with DEA/NO (50 μM) for 20 min at 37 °C in the dark. As illustrated in Figure 2, wild-type iNOS is the only protein that exhibited a decrease in NO production (42 ± 2%) after reaction with DEA/NO, as compared to DEA. Wild-type protein, which contains a zinc tetrathiolate cluster, maintained 56% of its activity after 20 min at 37 °C (Figure 2 and Table 2). The cysteine tetrathiolate mutants C104A, C109A, and C104A/C109A showed no difference in activity between DEA- and DEA/NO-treated samples, indicating that an intact zinc tetrathiolate cluster is required for NO-mediated loss in activity. The catalytic activity in the mutants was considerably decreased from samples that were kept at 4 °C (Table 2). The two single mutants, C104A and C109A, retain ~6% of their original activity after 20 min at 37 °C. This suggests that little protein in these assays contained an interchain disulfide; however, none was detected by MS (see below). The double mutant retained only 1.3% of the original activity.

Preparation of Biotinylated iNOS$_{heme}$ and Sensitivity of NeutrAvidin-HRP. To assess the detection limit of the biotin switch method, the heme domain of iNOS was biotinylated using the thiol-specific reagent, biotin-HPDP, as described in the Experimental Procedures section. Reaction progress

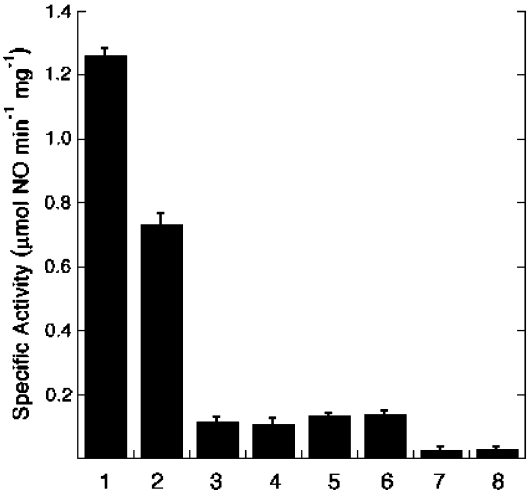

FIGURE 2: Assay of iNOS activity. The oxyHb assay was used to measure the activity of the wild type, C104A, C109A, and the C104A/C109A double mutant of iNOS after treatment with DEA or DEA/NO (50 μM) for 20 min in the dark at 37 °C. These samples were then diluted into the activity assay buffer, and the increase in A_{401} (metHb) was measured. Final protein concentration was 15 nM. The specific activity is expressed as μmol of NO min^{-1} mg^{-1}. The error is expressed as standard deviation and is from three separate measurements. Sample assignments: 1, wild type + DEA; 2, wild type + DEA/NO; 3, C104A + DEA; 4, C104A + DEA/NO; 5, C109A + DEA; 6, C109A + DEA/NO; 7, C104A/C109A + DEA; 8, C104A/C109A + DEA/NO.

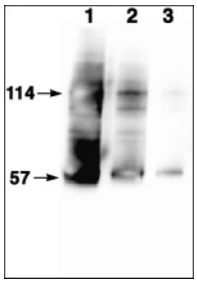

FIGURE 3: Confirmation of iNOS$_{heme}$ biotinylation and determination of detection limit. The heme domain of iNOS was S-biotinylated as described and separated by nonreducing SDS−PAGE. The gel was then transferred to a nitrocellulose membrane and blocked overnight in 3% BSA before detection by NeutrAvidin-HRP (Pierce). Monomeric iNOS$_{heme}$ (57 kDa) and the disulfide cross-linked dimer are visible (114 kDa). Lane assignments: 1, 300 ng; 2, 30 ng; 3, 3.0 ng. The sensitivity limit is estimated to be ~1 ng using chemiluminescent detection.

was monitored using UV−vis spectrophotometry at 343 nm, which indicated that approximately 4 mol of biotin-HPDP had reacted with the iNOS$_{heme}$ monomer (data not shown). Since no other thiols were in solution during this reaction, it is probable that most of the biotinylating reagent consumed actually reacted with reduced cysteines of iNOS$_{heme}$ (11 cysteines in iNOS$_{heme}$). After removal of excess biotin-HPDP by a PD-10 desalting column, protein biotinylation was confirmed by a Western blot using NeutrAvidin-HRP. The detection limit under our conditions is approximately 1 ng of biotinylated iNOS$_{heme}$ (Figure 3).

Nitrosothiols Present on iNOS after Treatment with DEA/NO. The biotin switch method, developed by Jaffrey and Snyder (*38*), is a sensitive assay for the detection of protein nitrosothiols. We used this assay with slight modifications to examine S-nitrosation of iNOS after reaction with 50 μM NO donor, DEA/NO. Wild-type iNOS treated with DEA/

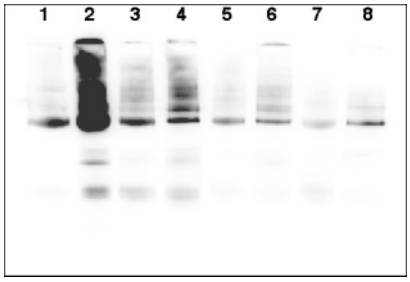

FIGURE 4: The biotin switch method on iNOS and the cysteine mutants. Samples for the assay were treated using the modified protocol described using DEA or DEA/NO (50 μM). The outcome of the assay is an exchange of protein nitrosothiols for a disulfide-bound biotin. Samples were separated by SDS−PAGE and transferred to a nitrocellulose membrane. After overnight blocking, the blot was probed with NeutrAvidin-HRP, and biotinylation was detected by chemiluminescence. Protein aggregation can be seen at the top of the membrane and small amounts of nonenzymatic proteolysis toward the lower half. Lane assignments: 1, wild-type iNOS DEA; 2, wild-type iNOS DEA/NO; 3, C104A DEA; 4, C104A DEA/NO; 5, C109A DEA; 6, C109A DEA/NO; 7, C104A/C109A DEA; 8, C104A/C109A DEA/NO.

NO gave a strong signal by Western blot. Using DEA as a negative control at an equal concentration, we observed that a portion of iNOS as isolated is S-nitrosated (Figure 4). Since the purification steps include all of the cofactors and substrates required for catalysis, NO is formed during the isolation and would be capable of S-nitrosation chemistry. When the in vitro S-nitrosation step of the biotin switch method was performed anaerobically, no increase in S-biotinylation was observed above controls with the addition of DEA/NO, demonstrating an oxygen requirement for the nitrosation chemistry (data not shown).

MALDI MS Analysis of S-Nitrosated iNOS. To map the cysteine(s) that undergo S-biotinylation during the biotin switch method, the proteins that were treated with DEA and DEA/NO were proteolytically digested. With the large size of the iNOS monomer, 130 kDa not including the associated CaM, a tryptic digest yields several peptide fragments with masses that are nearly identical to one another. More importantly, the mass of suspected biotinylated peptides would match the mass of other fragments that were not expected to be biotinylated. Since a goal was to sequence the modified peptides via tandem MS, LysC digestions were used. Peptides from LysC digestion were of sufficiently different masses so that the peptides could be selectively sent to a collision cell for CID measurements without further purification.

The sequence of the zinc-binding region of iNOS is $_{104}$CKSKSC$_{109}$ and contains two potential sites for LysC cleavage. Using LysC, we were able to distinguish between C104 and C109 S-biotinylation. As shown in Figure 5, masses were identified as S-biotinylated peptides 98−105 (1300.5756 Da) and 108−117 (1477.7065 Da) on an internally calibrated MALDI MS spectrum of the LysC digest. Disulfide formation is known to compete with nitrosothiols on neighboring cysteines (*52*, *53*), but no intra- or interchain disulfides with C104 or C109 were found by MALDI under nonreducing conditions.

Peptides from other proteolytic digests (trypsin and AspN) of iNOS after treatment with the biotin switch method were purified by using immobilized streptavidin (agarose beads) and then analyzed by MALDI MS. The mass spectra from these digests contained several peptides of interest that could correspond to biotinylation of peptides containing C104 and C109. The spectra also contain several unidentified peaks. These peaks could result from the cleavage of streptavidin, nonspecific binding (which can be reduced but not eliminated by stringent washing), and/or nonspecific proteolysis. The trypsin digest and streptavidin−agarose-enriched spectra are shown in the Supporting Information.

Tandem MALDI MS was used to sequence two peptides of interest (1300.51 and 1477.66 Da) from the LysC digestion. The CID spectra from the peptides are shown in Figures 6 and 7. The 1300.51 Da peptide gave a complete y^+ ion series and most of the b^+ ions. The biotin tag also dissociated from the peptide (431.19, molecular ion; 463.14, molecular ion plus cysteine sulfur), providing a set of diagnostic mass peaks to check for other biotinylated peptides. The CID spectrum for the 1477.66 Da peptide contained most of the y^+ and b^+ ions in addition to the same biotin tag fragments. These spectra confirm the identity of the peptides as ATSDFTCK (1300.51 Da) and SCLGSIMNPK (1477.66 Da).

The iNOS digest was searched for other peptides that could potentially contain a S-biotinylated cysteine. The trypsin and AspN digestions were also surveyed in order to increase sequence coverage. Between the three proteases, 100% of the iNOS sequence was accounted for in the MALDI spectra. We were unable to confirm biotinylation of any other cysteines in the full-length protein. However, a very low intensity mass at 4166.11 Da from a LysC digestion was detected that may correspond to S-biotinylated 1057−1090 (contains C1076; data not shown). Unfortunately, the low abundance of this ion precluded CID sequencing. This mass was not observed in the streptavidin-purified sample from a trypsin digest, but this does not exclude the possibility of a minor S-nitrosation site.

Reaction of iNOS Cysteine Mutants with DEA/NO. The zinc tetrathiolate mutants of iNOS were reacted with DEA/NO under identical conditions as the wild type to establish a requirement for zinc in the nitrosation chemistry. None of the mutants displayed an increase above endogenous S-nitrosation. Conversely, the difference in signal between DEA and DEA/NO with the wild-type protein is clearly shown in lanes 1 and 2 (Figure 4). The double cysteine mutant still exhibited a low level of endogenous S-nitrosation, implying that either the zinc tetrathiolate cysteines are not the only S-nitrosated cysteines or MMTS blocking is not 100% efficient.

Endogenous S-Nitrosation of iNOS from RAW-264.7 Cells. To determine if iNOS was S-nitrosated within activated macrophages, RAW-264.7 cells were stimulated with IFN-γ and LPS for 24 h. Macrophages that were not stimulated do not make detectable iNOS by Western blot using a monoclonal antibody. After lysing the cells and immunoprecipitation of iNOS from the crude lysate, a portion of the sample was treated with $HgCl_2$ (3 mM, 40 °C, 30 min). Nitrosothiols are selectively and quantitatively reduced under these conditions. The protein samples (with or without $HgCl_2$ pretreatment) were taken through the biotin switch method (Figure 8). Only iNOS that was not pretreated shows a signal by Western blot after purification by immobilized streptavidin (SA) and elution with β-ME, which cleaves the reductively labile biotin tag from the protein. No exogenous NO was

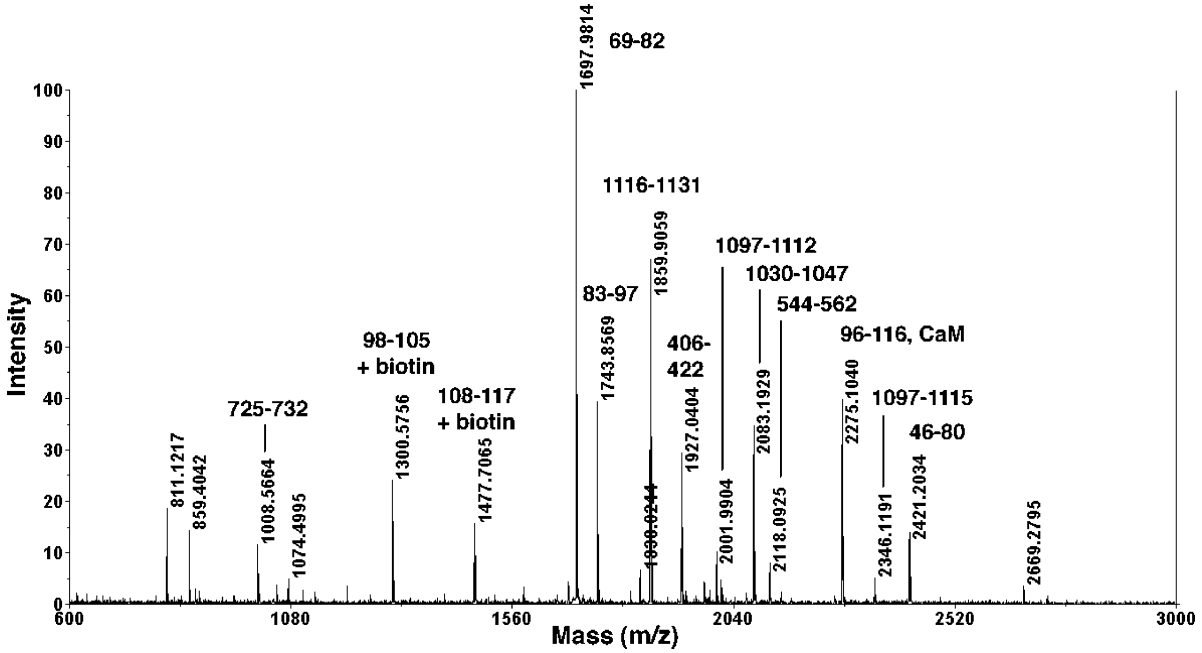

FIGURE 5: An internally calibrated MALDI MS spectrum from *m/z* 600−3000 of a LysC digest of wild-type iNOS. This sample (20 μg of iNOS) had been through the biotin switch method as described and subsequently digested with 267 ng of LysC at 37 °C for 5 h. After being desalted on C-18 ZipTips (Millipore), the samples were cospotted on the MALDI target with HCCA. The peaks at 1300.5756 Da (theoretical, 1300.5739 Da) and 1477.7065 Da (theoretical, 1477.7039 Da) were expected to correspond to biotin-HPDP-modified peptides 98−105 and 108−117, respectively. CaM, a peptide from calmodulin, copurifies with iNOS.

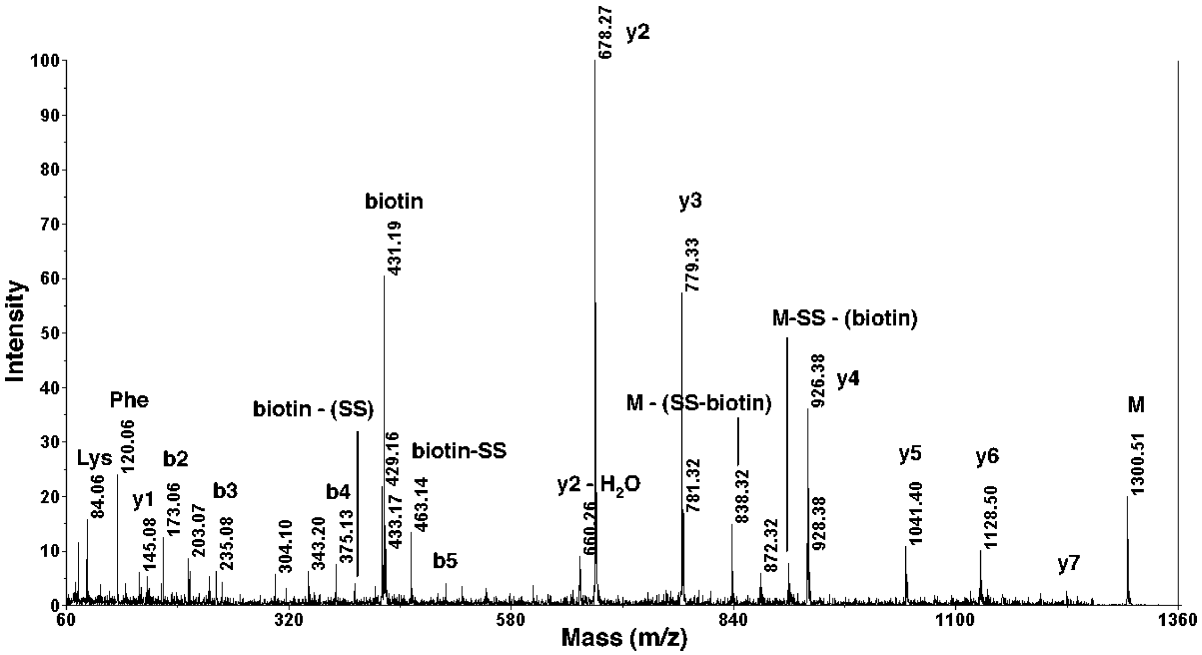

FIGURE 6: MALDI-TOF/TOF analysis of S-biotinylated peptide 98−105. The sample was prepared in an identical manner as samples for single TOF analysis. The CID spectrum of this 1300.5 Da peptide contains a complete y^+ series of ions, several of the b^+ ions, and peaks corresponding to the biotin tag. This spectrum confirms the identity of the peptide as S-biotinylated ATSDFTCK. Abbreviations: M, molecular ion; M-SS − (biotin), full peptide containing the disulfide but not the biotin; M − (SS-biotin), full peptide minus the cysteine sulfur and the disulfide-bound biotin; biotin, the biotin tag fragmented at the S−S bond; biotin − (SS), the biotin tag without sulfur; biotin-SS, the biotin tag with the cysteine sulfur.

added to these experiments; all of the NO produced was synthesized by iNOS. A pilot experiment without $HgCl_2$ pretreatment is included in the Supporting Information.

DISCUSSION

Three zinc tetrathiolate mutants of iNOS (C104A, C109A, and the double mutant C104A/C109A) were expressed in *E. coli* and purified to homogeneity (Supporting Information). ICP-AES and the PAR assay show that all of the cysteine mutants are purified without zinc whereas wild-type iNOS and the heme domain construct are purified with zinc content typical of an *E. coli* expression system (Table 1). Mutation of one of these zinc tetrathiolate cysteines causes the loss of two of the zinc-chelating sulfurs since the protein is homodimeric. The resulting structure yields a two-cysteine/two-alanine environment and is not capable of binding zinc.

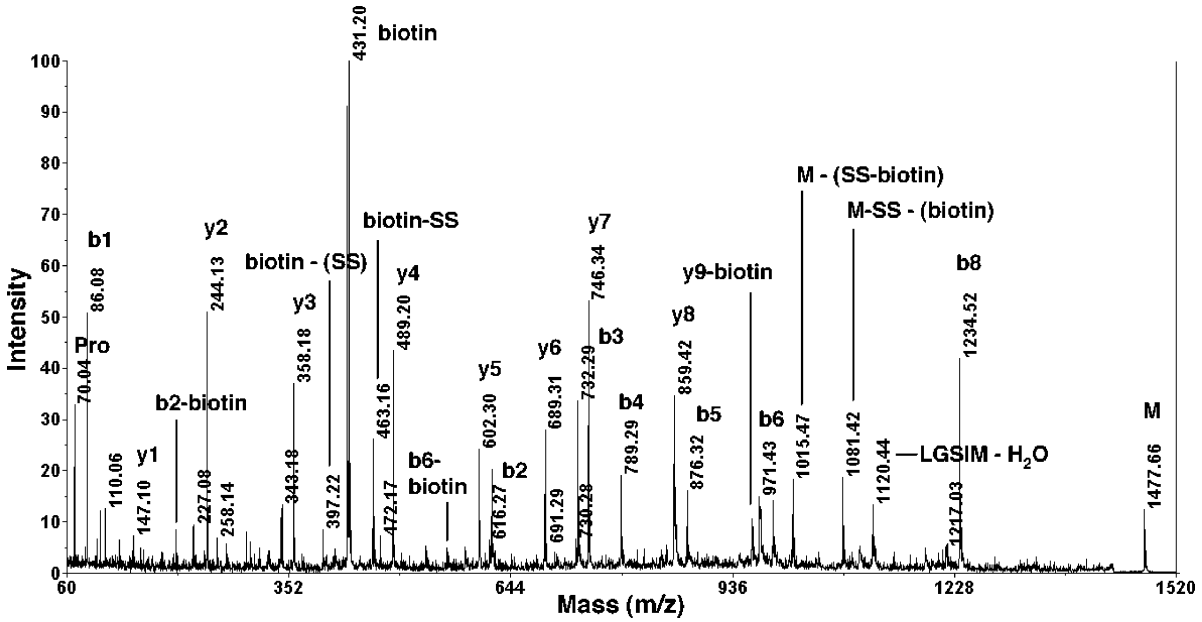

FIGURE 7: MALDI-TOF/TOF analysis of S-biotinylated peptide 108−117. The sample was prepared in an identical manner as samples for single TOF analysis. The CID spectrum of this 1477.7 Da peptide contains nearly all of the y^+ and b^+ ions with the biotin tag fragmenting in a similar manner as the 1300.5 Da peptide. An internal peak is also observed with loss of a water molecule, LGSIM. This spectrum confirms the identity as S-biotinylated SCLGSIMNPK. The abbreviation scheme is identical to that in Figure 6.

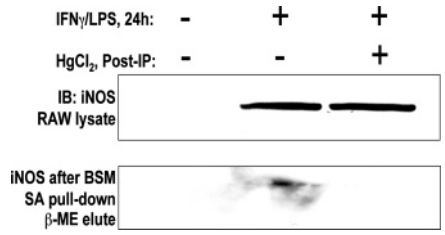

FIGURE 8: In vivo S-nitrosation of iNOS in macrophages. RAW-264.7 cells were activated for 24 h with *E. coli* LPS (35 ng/mL) plus recombinant murine IFN-γ (5 units/mL). The macrophages were then lysed, and iNOS was immunoprecipitated (IP) using a polyclonal antibody to iNOS and immobilized protein A (agarose beads). One sample of iNOS was pretreated with $HgCl_2$ (3 mM) to reduce the nitrosothiol before the biotin switch method was performed. The samples were then affinity purified by immobilized streptavidin (SA) (agarose beads), washed, and eluted with β-ME. Only samples with a disulfide-linked biotin are released with this methodology. All samples were then separated by SDS−PAGE, electroblotted to nitrocellulose, and probed with a monoclonal antibody for iNOS.

Likewise, the double mutant, a four-alanine environment, is also zinc free.

We initially expected that C104A and C109A would be purified as dimers, similar to wild type, and that the double cysteine mutant would be purified as a monomer. Our rationale for this was that while the single cysteine mutants would have reduced or no affinity for zinc, they both could still form an interchain disulfide, as observed in a crystal structure (*24*), whereas the C104A/C109A double mutant could not form an interchain disulfide. However, gel filtration showed that other contacts at the dimer interface are sufficient to hold the monomers together and the double mutant was also purified as a dimer. It is likely that only dimeric C104A/C109A is observed due to the fact that a very high, nonphysiological concentration of iNOS was loaded onto the column (~20 mg/mL) and the temperature was kept below 4 °C. The concentration of iNOS directly after gel filtration was ~5 mg/mL. At this high protein concentration, even a much larger monomer dissociation constant would still allow for the protein to be isolated as a dimer under these conditions.

Since dimerization of iNOS is a prerequisite for activity (*26*, *54*), a more sensitive method for determining the extent of iNOS monomerization is to measure protein activity. Using the oxyHb assay, the protein concentration is 4 orders of magnitude lower (15 nM) than that used for gel filtration. The double cysteine mutant was the only enzyme to exhibit a reduced rate of NO synthesis if all proteins were kept at 4 °C prior to the activity assay (Table 2). An increased K_D between iNOS monomers in the double mutant is likely a contributing factor to the loss in activity. The activity measurements suggest that the wild type and single tetrathiolate mutants of iNOS will have a dimer K_D much lower than 15 nM.

On the basis of gel filtration, the oxyHb assay, ICP-AES, and biotin switch method data shown in Figure 1, Figure 2, Table 3, and Figure 4, respectively, we hypothesize that NO can initiate iNOS monomer formation with concomitant release of zinc and protein S-nitrosation (Scheme 1). In an aerobic solution, NO and oxygen react in a rate-determining step (termolecular) to form NO_2. In a diffusion-limited step, NO and NO_2 recombine to form N_2O_3, a ^+NO donor. Cysteines ligated to zinc preferentially react with N_2O_3 with an equivalent of protein nitrosothiol and nitrite formed. Intramolecular transnitrosation reactions allow for any of the cysteines originally involved in zinc chelation to be S-nitrosated. A zinc dithiolate cluster is presumed to be unstable, and zinc is released from the dimer interface. Without the stabilizing zinc tetrathiolate cluster, the monomer dissociation constant is increased. iNOS then dissociates into its inactive monomeric form with either cysteine S-nitrosated, provided that the protein concentration is not abnormally high. It is important to note that even though zinc-free mutants of iNOS can be purified in dimeric form, conditions used to S-nitrosate the zinc tetrathiolate cysteines of wild-

Scheme 1: Proposed Mechanism of NO-Mediated S-Nitrosation of iNOS[a]

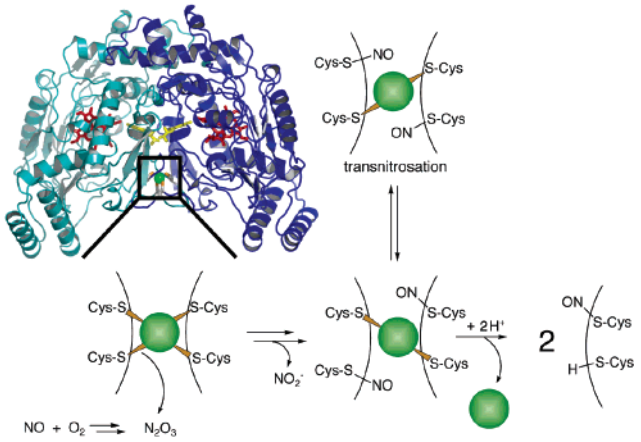

[a] The structure shown is the heme domain of iNOS, PDB ID 1NSI. The scheme shows the reaction of the zinc tetrathiolate cysteines with NO with the concomitant release of zinc (green sphere) and monomer formation.

type iNOS were sufficient to induce monomer formation and reduction in activity (Figures 1 and 2). Zinc tetrathiolate mutants do not exhibit a change in catalytic activity after exposure to DEA/NO, indicating that the S-nitrosation of the zinc tetrathiolate cysteines is responsible for the decrease in activity of the wild-type protein.

Pretreatment of any zinc tetrathiolate mutant at 37 °C for 20 min with DEA/NO or DEA resulted in a striking reduction in activity when compared to wild-type protein (Figure 2). S-Nitrosation cannot account for the decreased activity in the mutant proteins, as no change between the DEA/NO- and DEA-treated samples was observed. We attribute the reduction in mutant activity to an increased extent of monomer formation; the stabilizing zinc tetrathiolate cluster is not present. The activity of the single cysteine mutants (C104A and C109A) was significantly decreased compared to wild type but slightly higher than the C104A/C109A mutant. This is likely due to a small percentage of the single mutants forming an interchain disulfide, although none was detected by MS under nonreducing conditions.

Using the biotin switch method, we tested the proposed mechanism illustrated in Scheme 1. The hypothesis requires a zinc tetrathiolate cluster, which generates two highly reactive cysteine thiolates. Zinc tetrathiolate cysteines are much more reactive toward electrophiles, such as the nitrosating agent N_2O_3, than other cysteines in iNOS (24 cysteines/iNOS monomer). Coordination to zinc, a strong Lewis acid, has been shown to markedly decrease the pK_a of cysteine (from 8.5 to ~6), allowing the much more nucleophilic thiolate to predominate at physiological pH. Thiol ligation to zinc and the resulting increase in nucleophilicity have been demonstrated on metallothionein (*27*), alcohol dehydrogenase (*28*), and yeast farnesyltransferase (*31*). Ab initio calculations on metal-ligated cysteines have indicated that zinc and copper are quite efficient at thiol deprotonation (*32*). Therefore, we believe that the zinc tetrathiolate cysteines of iNOS can react with N_2O_3 with high chemoselectivity, provided the NO concentration is kept low. Using 50 μM DEA/NO, N_2O_3 is formed at a maximum velocity of ~700 nM N_2O_3 s^{-1}, but due to rapid hydrolysis in water, this concentration is never attained (*36*, *55*). As shown in Figure 4, only wild-type iNOS had increased levels of S-biotinylation after completion of the biotin switch method, indicating a requirement for zinc. Had much larger concentrations of NO been released, we expect the dependence on zinc to disappear because a significantly larger concentration of N_2O_3 would be formed. N_2O_3 formed under these conditions could then indiscriminately react with less nucleophilic amino acids (nonactivated reduced cysteines, tryptophans, histidines, lysines, and arginines) (*56*, *57*).

A small extent of S-biotinylation was also observed in the control samples (DEA) for the biotin switch method. This implies that, as purified, a detectable amount of iNOS could be S-nitrosated. An alternative explanation is that the MMTS blocking step did not go to completion. It is unlikely that S-nitrosation occurred during aerobic expression of the protein in *E. coli* since it is known that this organism does not have the ability to synthesize H_4B, and this cofactor is essential for NO synthesis (*15*, *44*, *58*). Additionally, *E. coli* growing in an aerobic environment do not produce NO (*59*). It appears that amounts of NO synthesized by iNOS during purification are sufficient for the observed S-nitrosation as all substrates and cofactors required for catalytic activity are present.

Our experiments using murine macrophages with no addition of exogenous NO enforce the above conclusion (Figure 8). These in vivo studies indicated that activated macrophages synthesize iNOS and a detectable amount of the enzyme was S-nitrosated. After the biotin switch method, we were only able to isolate iNOS with immobilized streptavidin if the samples were not pretreated with the selective nitrosothiol reducing agent, $HgCl_2$. Samples that were pretreated were reduced to the free thiol and subsequently blocked with MMTS. Derivatized as the methyl disulfide, these cysteines were unreactive to biotin-HPDP.

Utilizing MALDI-TOF and tandem TOF MALDI MS, we mapped the cysteines in the wild-type enzyme that were modified by S-biotinylation during the biotin switch method. We successfully and independently identified C104 and C109 as sites of S-biotinylation (Figures 6 and 7). However, this did not address the issue that the cysteine mutants and DEA controls were also modified to a much lower but detectable amount (by Western blot). Our attempts to locate the cysteine(s) that was (were) modified during the biotin switch method on the cysteine mutants were unsuccessful. The abundance of the S-biotinylated peptide was not high enough to give a signal in MALDI above noise.[2]

Reversible association with Ca^{2+}/CaM posttranslationally regulates the constitutive NOS isoforms (*21*, *22*). In contrast, iNOS association with CaM is considered nearly irreversible (*9*), and regulation occurs at the transcriptional level (*60*). Several hypotheses for posttranslational regulation of iNOS

[2] This is a reasonable assumption because of the superior sensitivity of the biotin switch method. We were able to detect ~1 ng of $iNOS_{heme}$ that was labeled four times with biotin-HPDP. A monolabeled protein would have a detection limit of ~4 ng. A complete LysC digestion of iNOS (150 kDa including CaM) yields peptides of an average molecular mass of 2 kDa. This would correspond to a total mass of only ~50 pg for the peptide of interest. Since the yield of each step in the biotin switch method is certainly not 100%, the mass of the peptide we were interested in sequencing could be present in low to subpicogram quantities. Given that the yield for each step in the biotin switch method is not quantitative, an alternative explanation for a weak signal by Western is from <100% MMTS blocking.

have been proposed, including arginine availability (*61*, *62*) and feedback inhibition by NO at the heme (*63*). On the basis of the results presented here, we conclude that another posttranslational modification, S-nitrosation, contributes to iNOS feedback regulation in vitro. S-Nitrosation of the zinc tetrathiolate cysteines in iNOS stimulates zinc release from the dimer interface, resulting in monomer formation and reduction in catalytic activity due to a larger monomer dissociation constant. The in vivo studies using mouse macrophages demonstrate that NO produced by iNOS in cell culture is sufficient to yield detectable S-nitrosated protein via the biotin switch method. Further work is necessary to establish a link between our in vitro results and NO-mediated deactivation of iNOS in vivo. The data presented here suggest that it may be crucial for macrophages to either repair the S-nitrosated iNOS or synthesize new iNOS since this protein must function in a chemically harsh environment.

ACKNOWLEDGMENT

We thank Scott D. Luzzi for help in purifying iNOS from *E. coli*, Steve A. Mills for assisting with ICP-AES measurements, Arnie Falick for acquiring the tandem MS spectra, and members of the Marletta laboratory for critical review of the manuscript.

SUPPORTING INFORMATION AVAILABLE

Four figures showing SDS−PAGE of iNOS, MALDI MS spectra of a trypsin digest of iNOS and RAW pilot experiment. This material is available free of charge via the Internet at http://pubs.acs.org.

REFERENCES

1. Pufahl, R. A., Nanjappan, P. G., Woodard, R. W., and Marletta, M. A. (1992) Mechanistic probes of N-hydroxylation of L-arginine by the inducible nitric oxide synthase from murine macrophages, *Biochemistry 31*, 6822−6828.
2. Stuehr, D. J., Kwon, N. S., Nathan, C. F., Griffith, O. W., Feldman, P. L., and Wiseman, J. (1991) N^{ω}-hydroxy-L-arginine is an intermediate in the biosynthesis of nitric oxide from L-arginine, *J. Biol. Chem. 266*, 6259−6263.
3. White, K. A., and Marletta, M. A. (1992) Nitric oxide synthase is a cytochrome P-450 type hemoprotein, *Biochemistry 31*, 6627−6631.
4. Stuehr, D. J., and Ikeda-Saito, M. (1992) Spectral characterization of brain and macrophage nitric oxide synthases. Cytochrome P-450-like hemeproteins that contain a flavin semiquinone radical, *J. Biol. Chem. 267*, 20547−20550.
5. McMillan, K., Bredt, D. S., Hirsch, D. J., Snyder, S. H., Clark, J. E., and Masters, B. S. (1992) Cloned, expressed rat cerebellar nitric oxide synthase contains stoichiometric amounts of heme, which binds carbon monoxide, *Proc. Natl. Acad. Sci. U.S.A. 89*, 11141−11145.
6. Hevel, J. M., White, K. A., and Marletta, M. A. (1991) Purification of the inducible murine macrophage nitric oxide synthase. Identification as a flavoprotein, *J. Biol. Chem. 266*, 22789−22791.
7. Stuehr, D. J., Cho, H. J., Kwon, N. S., Weise, M. F., and Nathan, C. F. (1991) Purification and characterization of the cytokine-induced macrophage nitric oxide synthase: an FAD- and FMN-containing flavoprotein, *Proc. Natl. Acad. Sci. U.S.A. 88*, 7773−7777.
8. Mayer, B., John, M., Heinzel, B., Werner, E. R., Wachter, H., Schultz, G., and Bohme, E. (1991) Brain nitric oxide synthase is a biopterin- and flavin-containing multi-functional oxido-reductase, *FEBS Lett. 288*, 187−191.
9. Schmidt, H. H., Smith, R. M., Nakane, M., and Murad, F. (1992) Ca^{2+}/calmodulin-dependent NO synthase type I: a biopteroflavoprotein with Ca^{2+}/calmodulin-independent diaphorase and reductase activities, *Biochemistry 31*, 3243−3249.
10. Marletta, M. A., Hurshman, A. R., and Rusche, K. M. (1998) Catalysis by nitric oxide synthase, *Curr. Opin. Chem. Biol. 2*, 656−663.
11. Alderton, W. K., Cooper, C. E., and Knowles, R. G. (2001) Nitric oxide synthases: structure, function and inhibition, *Biochem. J. 357*, 593−615.
12. Cho, H. J., Xie, Q. W., Calaycay, J., Mumford, R. A., Swiderek, K. M., Lee, T. D., and Nathan, C. (1992) Calmodulin is a subunit of nitric oxide synthase from macrophages, *J. Exp. Med. 176*, 599−604.
13. Forstermann, U., Pollock, J. S., Schmidt, H. H., Heller, M., and Murad, F. (1991) Calmodulin-dependent endothelium-derived relaxing factor/nitric oxide synthase activity is present in the particulate and cytosolic fractions of bovine aortic endothelial cells, *Proc. Natl. Acad. Sci. U.S.A. 88*, 1788−1792.
14. Sheta, E. A., McMillan, K., and Masters, B. S. (1994) Evidence for a bidomain structure of constitutive cerebellar nitric oxide synthase, *J. Biol. Chem. 269*, 15147−15153.
15. Crane, B. R., Arvai, A. S., Ghosh, D. K., Wu, C., Getzoff, E. D., Stuehr, D. J., and Tainer, J. A. (1998) Structure of nitric oxide synthase oxygenase dimer with pterin and substrate, *Science 279*, 2121−2126.
16. Raman, C. S., Li, H., Martasek, P., Kral, V., Masters, B. S., and Poulos, T. L. (1998) Crystal structure of constitutive endothelial nitric oxide synthase: a paradigm for pterin function involving a novel metal center, *Cell 95*, 939−950.
17. Garcin, E. D., Bruns, C. M., Lloyd, S. J., Hosfield, D. J., Tiso, M., Gachhui, R., Stuehr, D. J., Tainer, J. A., and Getzoff, E. D. (2004) Structural basis for isozyme-specific regulation of electron transfer in nitric-oxide synthase, *J. Biol. Chem. 279*, 37918−37927.
18. Zhang, J., Martasek, P., Paschke, R., Shea, T., Siler Masters, B. S., and Kim, J. J. (2001) Crystal structure of the FAD/NADPH-binding domain of rat neuronal nitric-oxide synthase. Comparisons with NADPH-cytochrome P450 oxidoreductase, *J. Biol. Chem. 276*, 37506−37513.
19. Cho, H. J., Martin, E., Xie, Q. W., Sassa, S., and Nathan, C. (1995) Inducible nitric oxide synthase: identification of amino acid residues essential for dimerization and binding of tetrahydrobiopterin, *Proc. Natl. Acad. Sci. U.S.A. 92*, 11514−11518.
20. Klatt, P., Schmidt, K., Lehner, D., Glatter, O., Bachinger, H. P., and Mayer, B. (1995) Structural analysis of porcine brain nitric oxide synthase reveals a role for tetrahydrobiopterin and L-arginine in the formation of an SDS-resistant dimer, *EMBO J. 14*, 3687−3695.
21. Panda, K., Ghosh, S., and Stuehr, D. J. (2001) Calmodulin activates intersubunit electron transfer in the neuronal nitric-oxide synthase dimer, *J. Biol. Chem. 276*, 23349−23356.
22. Zemojtel, T., Scheele, J. S., Martasek, P., Masters, B. S., Sharma, V. S., and Magde, D. (2003) Role of the interdomain linker probed by kinetics of CO ligation to an endothelial nitric oxide synthase mutant lacking the calmodulin binding peptide (residues 503−517 in bovine), *Biochemistry 42*, 6500−6506.
23. Hemmens, B., Goessler, W., Schmidt, K., and Mayer, B. (2000) Role of bound zinc in dimer stabilization but not enzyme activity of neuronal nitric-oxide synthase, *J. Biol. Chem. 275*, 35786−35791.
24. Li, H., Raman, C. S., Glaser, C. B., Blasko, E., Young, T. A., Parkinson, J. F., Whitlow, M., and Poulos, T. L. (1999) Crystal structures of zinc-free and -bound heme domain of human inducible nitric-oxide synthase. Implications for dimer stability and comparison with endothelial nitric-oxide synthase, *J. Biol. Chem. 274*, 21276−21284.
25. Ludwig, M. L., and Marletta, M. A. (1999) A new decoration for nitric oxide synthase—a Zn(Cys)4 site, *Struct. Folding Des. 7*, R73−R79.
26. Xie, Q. W., Leung, M., Fuortes, M., Sassa, S., and Nathan, C. (1996) Complementation analysis of mutants of nitric oxide synthase reveals that the active site requires two hemes, *Proc. Natl. Acad. Sci. U.S.A. 93*, 4891−4896.
27. Chen, Y., Irie, Y., Keung, W. M., and Maret, W. (2002) S-nitrosothiols react preferentially with zinc thiolate clusters of metallothionein III through transnitrosation, *Biochemistry 41*, 8360−8367.
28. Gergel, D., and Cederbaum, A. I. (1996) Inhibition of the catalytic activity of alcohol dehydrogenase by nitric oxide is associated with S nitrosylation and the release of zinc, *Biochemistry 35*, 16186−16194.

29. Maret, W. (2004) Zinc and sulfur: a critical biological partnership, *Biochemistry 43*, 3301−3309.
30. Ravi, K., Brennan, L. A., Levic, S., Ross, P. A., and Black, S. M. (2004) S-nitrosylation of endothelial nitric oxide synthase is associated with monomerization and decreased enzyme activity, *Proc. Natl. Acad. Sci. U.S.A. 101*, 2619−2624.
31. Rozema, D. B., and Poulter, C. D. (1999) Yeast protein farnesyltransferase. pK_as of peptide substrates bound as zinc thiolates, *Biochemistry 38*, 13138−13146.
32. Dudev, T., and Lim, C. (2002) Factors governing the protonation state of cysteines in proteins: an ab initio/CDM study, *J. Am. Chem. Soc. 124*, 6759−6766.
33. Zou, M. H., Shi, C., and Cohen, R. A. (2002) Oxidation of the zinc-thiolate complex and uncoupling of endothelial nitric oxide synthase by peroxynitrite, *J. Clin. Invest. 109*, 817−826.
34. MacMicking, J., Xie, Q. W., and Nathan, C. (1997) Nitric oxide and macrophage function, *Annu. Rev. Immunol. 15*, 323−350.
35. Xie, Q., and Nathan, C. (1994) The high-output nitric oxide pathway: role and regulation, *J. Leukocyte Biol. 56*, 576−582.
36. Wink, D. A., Nims, R. W., Darbyshire, J. F., Christodoulou, D., Hanbauer, I., Cox, G. W., Laval, F., Laval, J., Cook, J. A., Krishna, M. C., et al. (1994) Reaction kinetics for nitrosation of cysteine and glutathione in aerobic nitric oxide solutions at neutral pH. Insights into the fate and physiological effects of intermediates generated in the NO/O_2 reaction, *Chem. Res. Toxicol. 7*, 519−525.
37. Jourd'heuil, D., Jourd'heuil, F. L., and Feelisch, M. (2003) Oxidation and nitrosation of thiols at low micromolar exposure to nitric oxide. Evidence for a free radical mechanism, *J. Biol. Chem. 278*, 15720−15726.
38. Jaffrey, S. R., and Snyder, S. H. (2001) The biotin switch method for the detection of S-nitrosylated proteins, *Sci. STKE 2001*, PL1.
39. Rogers, N. E., and Ignarro, L. J. (1992) Constitutive nitric oxide synthase from cerebellum is reversibly inhibited by nitric oxide formed from L-arginine, *Biochem. Biophys. Res. Commun. 189*, 242−249.
40. Buga, G. M., Griscavage, J. M., Rogers, N. E., and Ignarro, L. J. (1993) Negative feedback regulation of endothelial cell function by nitric oxide, *Circ. Res. 73*, 808−812.
41. Ma, X. L., Lopez, B. L., Christopher, T. A., Birenbaum, D. S., and Vinten-Johansen, J. (1996) Exogenous NO inhibits basal NO release from vascular endothelium in vitro and in vivo, *Am. J. Physiol. 271*, H2045−H2051.
42. Zhang, J., Li, Y. D., Patel, J. M., and Block, E. R. (1998) Thioredoxin overexpression prevents NO-induced reduction of NO synthase activity in lung endothelial cells, *Am. J. Physiol. 275*, L288−L293.
43. Shao, L. E., Tanaka, T., Gribi, R., and Yu, J. (2002) Thioredoxin-related regulation of NO/NOS activities, *Ann. N.Y. Acad. Sci. 962*, 140−150.
44. Rusche, K. M., Spiering, M. M., and Marletta, M. A. (1998) Reactions catalyzed by tetrahydrobiopterin-free nitric oxide synthase, *Biochemistry 37*, 15503−15512.
45. Hurshman, A. R., and Marletta, M. A. (2002) Reactions catalyzed by the heme domain of inducible nitric oxide synthase: evidence for the involvement of tetrahydrobiopterin in electron transfer, *Biochemistry 41*, 3439−3456.
46. Hevel, J. M., and Marletta, M. A. (1994) Nitric-oxide synthase assays, *Methods Enzymol. 233*, 250−258.
47. Kim, J. E., and Tannenbaum, S. R. (2004) S-Nitrosation regulates the activation of endogenous procaspase-9 in HT-29 human colon carcinoma cells, *J. Biol. Chem. 279*, 9758−9764.
48. Perry, J. M., Moon, N., Zhao, Y., Dunham, W. R., and Marletta, M. A. (1998) The high-potential flavin and heme of nitric oxide synthase are not magnetically linked: implications for electron transfer, *Chem. Biol. 5*, 355−364.
49. Miller, R. T., Martasek, P., Raman, C. S., and Masters, B. S. (1999) Zinc content of *Escherichia coli*-expressed constitutive isoforms of nitric-oxide synthase. Enzymatic activity and effect of pterin, *J. Biol. Chem. 274*, 14537−14540.
50. Fischmann, T. O., Hruza, A., Niu, X. D., Fossetta, J. D., Lunn, C. A., Dolphin, E., Prongay, A. J., Reichert, P., Lundell, D. J., Narula, S. K., and Weber, P. C. (1999) Structural characterization of nitric oxide synthase isoforms reveals striking active-site conservation, *Nat. Struct. Biol. 6*, 233−242.
51. Crow, J. P., Sampson, J. B., Zhuang, Y., Thompson, J. A., and Beckman, J. S. (1997) Decreased zinc affinity of amyotrophic lateral sclerosis-associated superoxide dismutase mutants leads to enhanced catalysis of tyrosine nitration by peroxynitrite, *J. Neurochem. 69*, 1936−1944.
52. Crow, J. P., and Beckman, J. S. (1995) Reactions between nitric oxide, superoxide, and peroxynitrite: footprints of peroxynitrite in vivo, *Adv. Pharmacol. 34*, 17−43.
53. Zai, A., Rudd, M. A., Scribner, A. W., and Loscalzo, J. (1999) Cell-surface protein disulfide isomerase catalyzes transnitrosation and regulates intracellular transfer of nitric oxide, *J. Clin. Invest. 103*, 393−399.
54. Baek, K. J., Thiel, B. A., Lucas, S., and Stuehr, D. J. (1993) Macrophage nitric oxide synthase subunits. Purification, characterization, and role of prosthetic groups and substrate in regulating their association into a dimeric enzyme, *J. Biol. Chem. 268*, 21120−21129.
55. Wink, D. A., Darbyshire, J. F., Nims, R. W., Saavedra, J. E., and Ford, P. C. (1993) Reactions of the bioregulatory agent nitric oxide in oxygenated aqueous media: determination of the kinetics for oxidation and nitrosation by intermediates generated in the NO/O_2 reaction, *Chem. Res. Toxicol. 6*, 23−27.
56. Kuo, W. N., Ivy, D., Uruvadoo, L. G., White, A., and Graham, L. (2004) N-nitrosations of basic amino acid residues in polypeptide, *Front. Biosci. 9*, 3163−3166.
57. Suzuki, T., Mower, H. F., Friesen, M. D., Gilibert, I., Sawa, T., and Ohshima, H. (2004) Nitration and nitrosation of *N*-acetyl-L-tryptophan and tryptophan residues in proteins by various reactive nitrogen species, *Free Radical Biol. Med. 37*, 671−681.
58. Marletta, M. A. (1994) Nitric oxide synthase: aspects concerning structure and catalysis, *Cell 78*, 927−930.
59. Goretski, J., and Hollocher, T. C. (1990) The kinetic and isotopic competence of nitric oxide as an intermediate in denitrification, *J. Biol. Chem. 265*, 889−895.
60. Lowenstein, C. J., Alley, E. W., Raval, P., Snowman, A. M., Snyder, S. H., Russell, S. W., and Murphy, W. J. (1993) Macrophage nitric oxide synthase gene: two upstream regions mediate induction by interferon gamma and lipopolysaccharide, *Proc. Natl. Acad. Sci. U.S.A. 90*, 9730−9734.
61. El-Gayar, S., Thuring-Nahler, H., Pfeilschifter, J., Rollinghoff, M., and Bogdan, C. (2003) Translational control of inducible nitric oxide synthase by IL-13 and arginine availability in inflammatory macrophages, *J. Immunol. 171*, 4561−4568.
62. Aktan, F. (2004) iNOS-mediated nitric oxide production and its regulation, *Life Sci. 75*, 639−653.
63. Gautier, C., Negrerie, M., Wang, Z. Q., Lambry, J. C., Stuehr, D. J., Collin, F., Martin, J. L., and Slama-Schwok, A. (2004) Dynamic regulation of the inducible nitric-oxide synthase by NO: comparison with the endothelial isoform, *J. Biol. Chem. 279*, 4358−4365.

BI0474463